MARSHALL
GRANT
IN-32-CR
199126
74 P.

THEORETICAL INVESTIGATION OF EM WAVE GENERATION AND

RADIATION IN THE ULF, ELF, AND VLF BANDS BY THE

ELECTRODYNAMIC ORBITING TETHER

GRANT NAG8-638

Final Report

For the period 1 May 1987 through 31 July 1988

Principal Investigator

Dr. Robert D. Estes

March 1989

Prepared for
National Aeronautics and Space Administration
Marshall Space Flight Center, Alabama 35812

Smithsonian Institution
Astrophysical Observatory
Cambridge, Massachusetts 02138

The Smithsonian Astrophysical Observatory
is a member of the
Harvard-Smithsonian Center for Astrophysics

THEORETICAL INVESTIGATION OF EM WAVE GENERATION AND RADIATION IN THE ULF, ELF, AND VLF BANDS BY THE ELECTRODYNAMIC ORBITING TETHER

Grant NAG8-638

Final Report

For the period 1 May 1987 through 31 July 1988

Principal Investigator
Dr. Robert D. Estes

Co-Investigator
Dr. Mario D. Grossi

March 1989

The Smithsonian Astrophysical Observatory
is a member of the
Harvard-Smithsonian Center for Astrophysics

CONTENTS

1. INTRODUCTION

The problem of electromagnetic wave generation by an electrodynamic tethered satellite system is important both for the ordinary operation of such systems and for their possible application as orbiting transmitters. The tether's ionospheric "circuit closure" problem is closely linked with the propagation of charge-carrying electromagnetic wave packets away from the tethered system [Estes, 1988].

Previous analyses of the waves generated by large conductors moving through a magnetoplasma (in our case a tethered system moving through the ionosphere) [Drell, *et al.*, 1965; Belcastro, *et al.*, 1982; Rasmussen, *et al.*, 1985; Dobrowolny and Veltri, 1986; Barnett and Olbert, 1986; Estes, 1988] have considered the conductor to be immersed in an infinite plasma medium. When the boundary with the atmosphere is far enough away, this serves as a useful approximation for calculating the ionospheric waves and estimating their contribution to the tethered system's electrical impedance; but it tells us nothing about the electromagnetic signal one should expect to be associated with the tethered system in the atmosphere or on the Earth's surface. Heretofore there has not been a systematic treatment of the wave reflections and other effects of nonuniformities in the plasma medium. The inclusion of ion-neutral collisions introduces the possibility of coupling to other ionospheric wave modes. The work reported here represents a step towards a solution to the problem that takes into account the effects of boundaries and of vertical variations in plasma density, collision frequencies, and ion species.

Section 2 recapitulates the theory of Alfvén wave packet generation by an electrodynamic tethered system in an infinite plasma medium. A brief summary of

previous work on the problem, including an assessment of where things stand with regard to controversial points, is given there.

In Section 3 we present the generalization of our previous analysis that serves as the starting point—the incident wave–packet—for our treatment of the problem with boundaries and a nonuniform plasma.

We present the physics on which our method of attack is based in Section 4. There we have examined the consequences of the presence of the boundaries and the vertical nonuniformity of the ionosphere. One of the most significant new features to emerge when ion-neutral collisions are taken into account is the coupling of the Alfvén waves to the fast magnetosonic wave. This latter wave is important, as it may be confined by vertical variations in the Alfvén speed to a sort of leaky ionospheric wave guide (centered at plasma density maximum in the F-layer), the resonances of which could be of great importance to the signal received on the Earth's surface. We take the infinite medium solution for the case where the (uniform) geomagnetic field makes an arbitrary angle with the vertical as the incident wave–packet. Even without a full solution, a number of conclusions can be drawn, the most important of which may be that the electromagnetic field associated with the operation of a *steady-current* tethered system will probably be too weak to detect on the Earth's surface, even for large tether currents. This is due to the total reflection of the incident wave at the atmospheric boundary and the inability of a steady-current tethered system to excite the ionospheric wave-guide.

An outline of our approach to the numerical problem is then given in Section 5. Given our conclusions about the weakness of the steady-current signal on the Earth's

surface, we consider slowly varying tether currents.. We propose to use numerical integrations and boundary conditions consistent with a conducting Earth to obtain the solution for the horizontal electromagnetic field components at the boundary of the ionosphere with the atmospheric cavity. The proposed method, which is rather complicated, involves the use of Budden admittance matrices to take into account the incident and reflected Alfvén waves and the fast magnetosonic wave to which the Alfvén waves are coupled. We have begun software development for this project and plan to continue work on this problem under another NASA contract.

A summary of our conclusions and planned future work is found in Section 6.

2. REVIEW OF PREVIOUS RESULTS ON TETHER WAVE GENERATION

The theory developed in the prior Smithsonian Astrophysical Observatory (SAO) study of electromagnetic wave generation by an electrodynamic tether is reported in detail in the NASA report NAG8-551. A slightly modified version of a section of the report appeared in *The Journal of Geophysical Research* [Estes, 1988]. The publication of the results enables us to consider them in the light of the response they have received from other investigators in the field.

Our study built upon previous ones [Barnett and Olbert, 1986; Belcastro et al., 1982; Dobrowolny and Veltri, 1986; Drell et al., 1965; Rasmussen et al., 1985] but sought to obtain more believable results by using a more realistic model for the electric current distribution of the electrodynamic tether. Previous investigators had modeled the tether current system as a long cylinder. They had either considered an orbiting canister with a dimension along the direction of flight measured in tens of meters or, at the other extreme, an orbiting wire. Neither approach took into account the peculiar dumbbell shape of a tethered satellite system, which consists of a long, narrow wire terminated by satellites (or plasma clouds) with dimensions along the direction of motion that are much greater than the tether diameter. The SAO study showed that the orbiting canister approach, although it had not been thoroughly justified before, should provide a reasonable approximation for the purposes of calculating the wave impedance and ionospheric currents associated with steady-state (constant current) operation of an electrody-

namic tethered satellite system, provided that the current distribution assumes a constant value along the length of the tether, i.e., an insulated tether is assumed. This is true because it is primarily the changing fields associated with the injection of charge into the ionosphere at the ends of the moving system that drive the electromagnetic waves. Thus, any two moving systems that inject charge into the ionosphere at the same rate over the same area are equivalent from the standpoint of wave generation. By the same token, the orbiting wire model was found to be a poor model for an electrodynamic tether because it undervalued the dimensions of the terminating, charge-exchanging parts of the system by orders of magnitude.

Barnett and Olbert [1986] of MIT had used calculations based on an orbiting wire model to advance the idea that the wave impedance associated with the operation of a constant current electrodynamic tethered satellite system would be on the order of 10,000 to 100,000 Ohms, as opposed to previous estimates on the order of an Ohm. This was not an academic question, since such high impedance values would have precluded the use of tethered systems for any applications that required substantial currents. This conflict has now been resolved, and Barnett and Olbert have acknowledged that their use of the orbiting wire model led to a great overestimation of the wave impedance associated with the frequency band lying between the lower hybrid frequency and the electron cyclotron frequency. In a private communication they expressed complete agreement with the SAO study on this point, and in a recent publication [Barnett et al., 1988] they credit R. Estes with pointing out that it is only the

system/ionosphere charge-exchange region that matters for wave excitation within the steady-state, cold plasma models considered up until now.

Agreement has not yet been reached with M. Dobrowolny and his Italian colleagues on a number of points, which involve the functional dependence of the Alfvén wave impedance on the Alfvén and satellite velocities as well as the system dimensions. The SAO study, in agreement with all other studies but that of Dobrowolny and Veltri [1986] found that this impedance varies linearly with the Alfvén speed, while being independent of the satellite velocity within the approximations used. Dobrowolny and Veltri, however, had found an inverse dependence on the Alfvén speed and a quadratic dependence on the satellite speed. They have based their defense of these results largely on the thesis that the quadratic dependence on the satellite speed is much more reasonable physically, since the effect disappears (as it should) if the system is not moving.

We will only sketch the argument here. The details of their argument and our rebuttal can be found in the Appendix. The Dobrowolny paper also contained a physical argument to explain the divergence of their results from those in the 1965 work of Drell, et al. We have already pointed out flaws in that argument [Estes, 1988]. The Italian investigators still have not addressed the question of why their results differed from all of the other prior studies as well, studies which obtained quite different results from those of Drell, et al. and which are in fact the relevant comparisons. Although Dobrowolny and his co-workers

have not emphasized this part of their results, the linear dependence of the Alfvén wave impedance on the tether length that they found is as important a difference from the results of other investigators as the inverse dependence on the Alfvén speed is.

Basically, Dobrowolny and his colleagues maintain that the bulk of the plasma current is a "dc" current having nothing to do with wave phenomena. We argue that this amounts to saying that a current pulse traveling down a transmission line is a dc current. This approach appears fundamentally wrong when dealing with plasma currents, which are essentially wave phenomena.

Our analysis has shown how the excitation of Alfvén waves as the dominant form of radiation depends on the dimension along the line-of-flight of the charge-exchange region between the system and the ionosphere. It was the fact that this dimension is necessarily on the order of meters that enabled us to discard the higher frequency radiation that Barnett and Olbert were then arguing to be important. The vanishingly small dimension used by Dobrowolny and Veltri should lead to the same swamping of the Alfvén band by the lower hybrid band radiation observed by Barnett and Olbert in their orbiting wire calculations, but since Dobrowolny and Veltri are only looking at Alfvén waves they do not deal with this issue.

Having failed to find an error in the straightforward SAO analysis, Dobrowolny and his colleague Iess advanced physical arguments about why the

SAO analysis could not be right. They maintain that their result makes sense physically because there is an explicit quadratic dependence on the velocity of the satellite in their expression for the wave impedance, while the SAO result (they argue) does not go to zero as v_z does.

In the Appendix we demonstrate that our analysis also gives zero contribution to the wave impednace when the velocity is zero. The question is then: for a given non-zero satellite velocity, what is the proper dependence for the wave impedance on the satellite velocity? We have found that the wave impedance is very similar to that for a bifilar transmission line and have argued that this makes physical sense. If one considers a real bifilar transmission line, the property of the medium between the two wires (which are electrically insulated from each other along their length—as the magnetic field lines effectively are in the ionosphere) which enters into the calculation is the dielectric constant. Now in the low frequency approximation, which is applicable to the case of Alfven waves, the dielectric constant of the plasma (the diagonal, perpendicular components of the dielectric tensor that is) is in fact independent of the frequency. That is, it is independent of the satellite velocity, which is the only source of time variation in the problem under consideration.

Thus the Alfvén wave impedance of an electrodynamic tethered satellite system should be roughly independent of the satellite velocity. We can see no argument at all that it should be quadratic in v_z, nor has anyone made a physical

argument for this particular functional form. We think this quadratic dependence found by Dobrowolny and Veltri is just the result of their having made an overly complicated analysis with some physically inconsistent assumptions. We demonstrate in the Appendix that, using the same starting point as the Italian investigators, we arrive again at our original results following two different routes.

Having carefully re-examined our earlier results, we proceed to them as a starting point for the solution to the problem of the propagation of tether-generated ionospheric waves.

3.   GENERALIZATION OF THE PREVIOUS RESULTS

Modeling of the electrodynamic tethered satellite system has heretofore been based on some unrealistic assumptions regarding uniformity of the plasma medium and constancy of the tether current. In addition, the simplest relationship has been chosen for the system velocity vector, magnetic field vector, and the vertical. These three directions have typically been taken to define a three-dimensional orthogonal system.

Taking into account the variations in plasma conductivity, density, collision frequencies, etc. in the ionosphere and the existence of the non-conducting atmosphere between the ionosphere and the earth will be the most difficult part of the process of obtaining a more realistic tether model. It will be an iterative project to solve the necessary boundary value problems. The analysis presented in this report is part of that project. Note that we use Gaussian units throughout our calculations.

As a first step, we generalize our previous results on steady-current tethers to the case of arbitrary angles between the vertical direction, the satellite velocity vector, and the magnetic field vector. Let us consider the case for which the geomagnetic field is not perpendicular to the vertical, but the orbital velocity vector of the system is perpendicular to the plane of the vertical and the magnetic field (See Figure 3.1). This would correspond to a system at the maximum

excursion in latitude for a non-equatorial orbit. Having previously demonstrated the equivalence of an orbiting "ribbon" current distribution and the idealized dumbbell tether current distribution used in the earlier analysis (NAG8-551), we can conveniently define the tether current distribution as

$$\vec{j} \; = \; \frac{\hat{y}'I}{L_x} \left[H(x' - L_x/2) - H(x' + L_x/2) \right]$$

$$\cdot \left[H(y' - L/2) - H(y' + L/2) \right] \delta(z') \tag{1}$$

where $x' = x - v_x t$ and $\hat{y}'$ lies along the vertical with $y' = 0$ at the middle of the tether. The $y - $ axis, which is orthogonal to $\vec{B}$ (the z axis) and $\vec{v}$ (the x axis) is indicated in Figure 3.1 as well. As in the previous analysis $H(x)$ is the Heaviside function defined by

$$H(x) = 1, \; x \geq 0$$
$$H(x) = 0, \; x < 0 \tag{2}$$

We now need $\vec{k} \cdot \vec{j}_k$, where $\vec{j}_k$ is the Fourier transform of the tether current density. This is most conveniently calculated in the x, y', z' co-ordinate system, where

$$\vec{k} \cdot \vec{j}_k \; = \; k_{y'} j_{y',k} \tag{3}$$
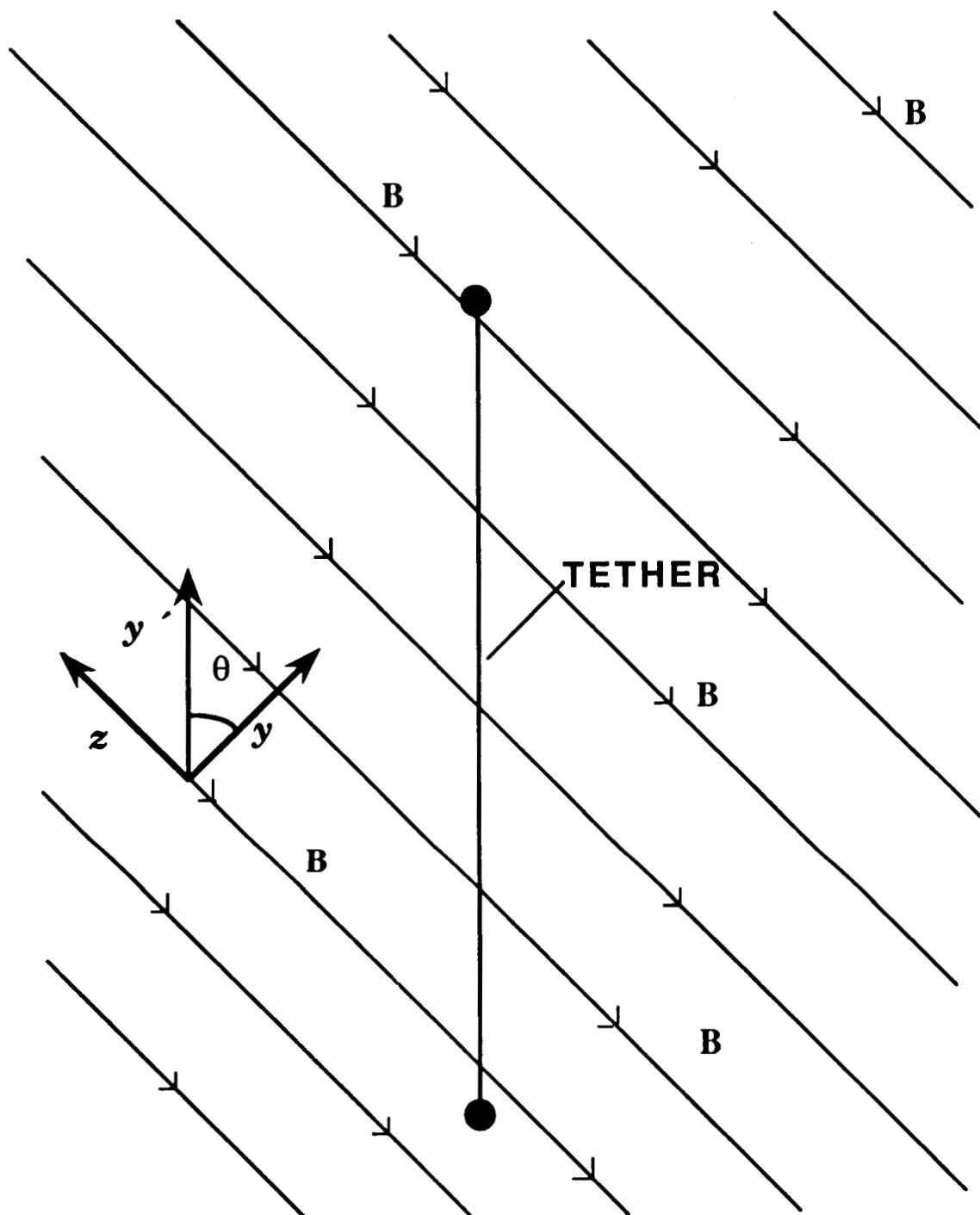
Motion of sytem (and x-axis) in out-of-page direction.
Tether along $y\,'$-axis

Figure 3.1.   Tethered system with non-horizontal magnetic field.

It is easy to obtain

$$j_{y',k} = \frac{2I}{\pi} \delta\left(\omega - k_z v_z\right) \frac{\sin k_z L_z/2}{k_z L_z} \frac{\sin k_{y'} L/2}{k_{y'}} \tag{4}$$

Thus

$$\vec{k} \cdot \vec{j} = \frac{2I}{\pi} \delta\left(\omega - k_z v_z\right) \frac{\sin(k_z L_z/2)}{k_z L_z} \sin(k_{y'} L/2) \tag{5}$$

Since

$$J_z = \frac{ic^2}{4\pi\omega} k_z \left(\vec{k} \cdot \vec{E}\right) \tag{6}$$

and

$$\vec{k} \cdot \vec{E} = \frac{4\pi i\omega}{c^2} \frac{\vec{k} \cdot \vec{j}}{\left(k_z{}^2 - \omega^2 \epsilon_\perp/c^2\right)} \tag{7}$$

have been obtained in the previous analysis, we can write the following expression

for the Fourier transform of the Alfvén wing or field-line sheet current:

$$J_z = \frac{-2I}{\pi} \quad \frac{k_z}{\left(k_z{}^2 - \omega^2 \epsilon_\perp/c^2\right)} \quad \sin\left(\frac{(k_y \cos\theta + k_z \sin\theta)L}{2}\right)$$

$$\cdot \frac{\sin(k_x L_x/2)}{k_x L_x} \delta(\omega - k_z v_z) \tag{8}$$

which differs from the earlier results for mutually orthogonal vectors only in the argument of one of the sine factors, which takes into account the dip angle of the magnetic field.

The problem is now to obtain the inverse Fourier transform of (8). The integrals over ω and k_y proceed very much as in the previous analysis, only with the results showing an obvious change due to the inclination of the magnetic field with respect to the horizontal. That is, the charge-exchange regions at the ends of the system are now located at $y = \pm \ (L/2) \cos\theta$. The integral over k_z also shows the effect of the magnetic field's inclination. The final integral over k_x takes the form

$$\frac{1}{2\pi L_x} \delta\left(y - L\cos\theta/2\right) \left[2H\left(z - L\sin\theta/2\right) - 1\right]$$

$$\cdot \int_0^{K_0} \frac{\sin(k_x L_x/2)}{k_x} \exp\left(ik_x[x' + (z - L\sin\theta/2)\alpha]\right) \ dk_x \tag{9}$$

$$- \frac{1}{2\pi L_x} \delta\left(y + L\cos\theta/2\right) \left[2H(z + L\sin\theta/2) - 1\right]$$

$$\cdot \int_0^{K_0} \frac{\sin(k_x L_x/2)}{k_x} \exp\left(ik_x[x' + (z + L\sin\theta/2)\alpha]\right) \ dk_x$$

where $\alpha = \left(\dfrac{v_z}{v_A}\right) \dfrac{1}{\left[\,1 \,-\, (k_z v_z/\Omega_{ci})^2\,\right]^{1/2}}$

Although this expression looks more complicated than the corresponding expression from the previous analysis, the basic content is the same. The Alfvén wings are seen to be field-line sheet currents at the ends of the system. The sign change in J_z occurs at the charge-exchange interface as before, but these are now located at $z = \pm (L/2) \sin\theta$. The top and bottom wings are connected by the condition of current continuity but otherwise they appear to be independent phenomena generated by the disturbances at their respective ends of the system. Except for the shift in lines of discontinuity in J_z to coincide with those traced by the charge exchange terminals, the Alfvén wing solutions are the same as before. The new solution clearly reduces to the old one when the angle θ goes to zero.

Another generalization of the previous analysis results when we allow for an arbitrary angle between the velocity vector of the system and the magnetic field lines. Let us consider the case when the tether lies along the vertical (y) axis and the magnetic field is in the horizontal plane antiparallel to the z-axis. The velocity vector, which lies in the horizontal plane, is allowed to be at an arbitrary angle φ with respect to the x-axis ((x,y,z) being a mutually orthogonal set of co-ordinate axes), as shown in Figure 3.2.

As before, the dimension of interest is that of the charge-exchange interface perpendicular to the magnetic field lines between the system and the plasma. For
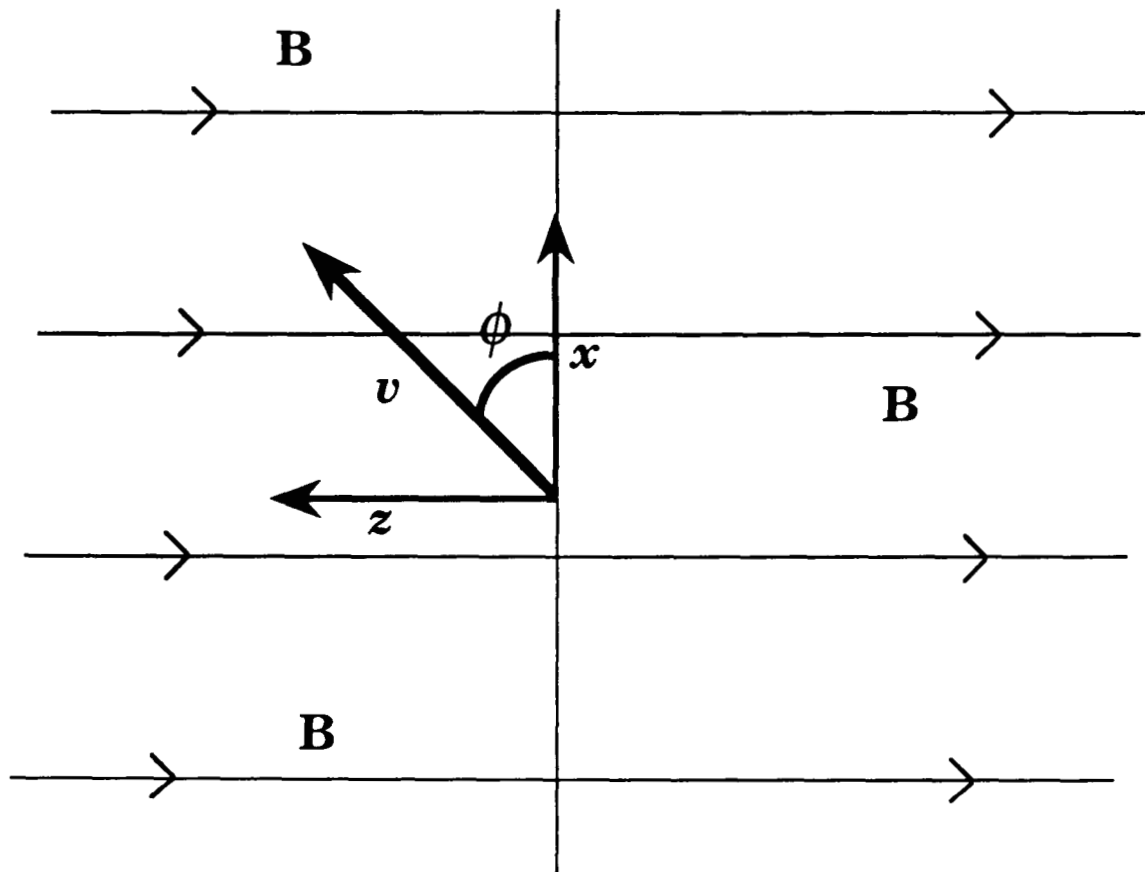
Figure 3.2. Tethered system geometry (viewed from below) for velocity vector not perpendicular to magnetic field.

a spherical terminating satellite this would be the same dimension L_z as before. The value of the current in the tether, assuming it to be induced strictly by the system's motion, would be reduced by the factor $\cos \varphi$ since the induced voltage depends on the component of the velocity perpendicular to $\vec{B}$. Our analysis is done in terms of the tether current I without calculating the value of I beforehand, but it is good to keep this difference in mind.

Once again we make use of the equivalence between an orbiting ribbon of current and the system under study to write the tether current density as

$$j_y = \frac{I}{L_z} \, \delta\Big(z - (v \sin \varphi)t\Big) \big[H(y - L/2) - H(y + L/2) \big]$$

$$\cdot \big[H(x' - L_z/2) - H(x' + L_z/2) \big] \tag{10}$$

where $x' = x - (v \cos \varphi)t$.

This leads to the Fourier transform result

$$\vec{k} \cdot \vec{j} = \frac{2I}{\pi} \, \delta(\omega - k_x v \sin \varphi - k_z v \cos \varphi) \sin\left(\frac{k_y L}{2}\right) \frac{\sin(k_z L_z/2)}{k_z L_z} \tag{11}$$

Our expression for the Fourier transform of J_z is identical to the previous one ((14) in our JGR paper) except for the changed argument of the delta function.

The integration over ω and k_y can proceed as in the *JGR* article. The singularities on the k_z real axis now occur at solutions of

$$k_z^2 = \left(\frac{v}{v_A}\right)^2 \frac{\left(k_x\cos\varphi + k_z\sin\varphi\right)^2}{\left(1 - (k_x\cos\varphi + k_z\sin\varphi)^2(v/\Omega_{ci})^2\right)} \tag{12}$$

From our previous results we can infer that, so long as φ is not too near $\pi/2$, the condition

$$\left|\, k_x\cos\varphi \,\right| \geq \left|\, k_z\sin\varphi \,\right| \tag{13}$$

should hold.

Then we obtain

$$k_z = \pm \frac{k_x v}{v_A} \frac{\cos\varphi}{\sqrt{1 - \left(k_x v\cos\varphi/\Omega_{ci}\right)^2}} \tag{14}$$

for the singularities; i.e., we just replace v_z with $v\cos\varphi$ in our previous analysis. The other change occurs in the complex exponentials left in the integrand

$$e^{\,ik_x(x - v\cos\varphi t)}e^{ik_z(z - v\sin\varphi t)}$$

After the integration over k_z we obtain

$$J_z(x',y,z') = \frac{1}{2\pi L_x} \left\{ \left[\delta(y - L/2) - \delta(y + L/2) \right] \right.$$

$$\left. \cdot \left[2H(z') - 1 \right] \cdot \int_0^{K_0} dk_x \frac{\sin(k_x L_x/2)}{k_x} \cdot e^{ik_x(x' + \alpha z')} \right\} \tag{15}$$

where $x' = x - vt \cos\varphi$,

$z' = -vt \sin\varphi$, and

$$\alpha = \frac{v \cos\varphi}{v_A \sqrt{1 - \left(k_x v \cos\varphi / \Omega_{ci} \right)^2}}$$

Without getting all the details, we can see that this implies Alfvén wings that look more or less like those shown in Figure 3.3. Seen from above it would appear as a winged structure flying along at an angle rather than "straight ahead."

There are a number of subtleties that would seem to be important, such as the actual shapes of the satellites, however, so that this analysis can only be viewed as a first approximation to an adequate description.
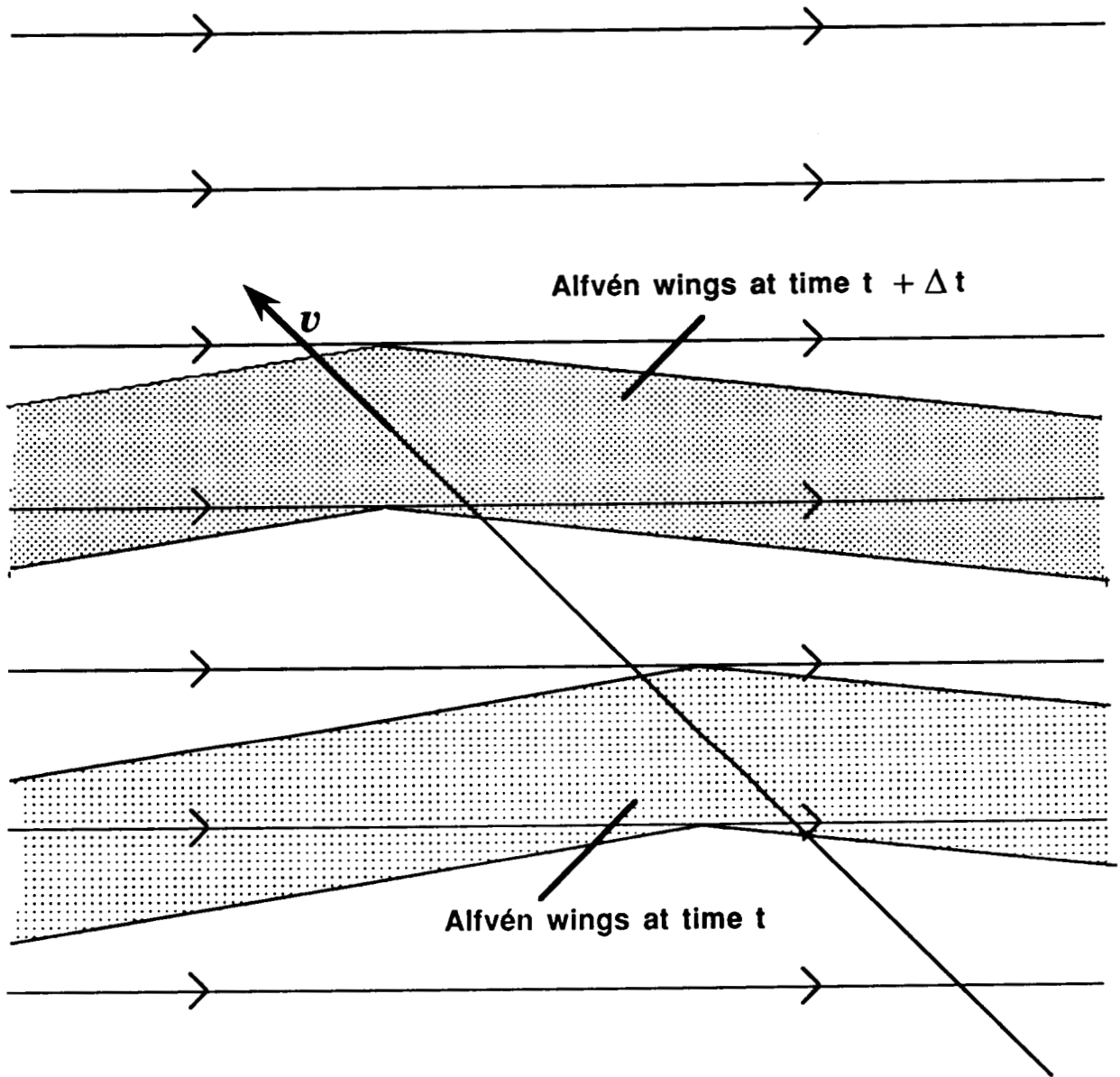
Figure 3.3. Alfvén wing motion (viewed from below) for velocity vector not
perpendicular to magnetic field.

4. ELECTRODYNAMIC TETHER IN A BOUNDED IONOSPHERE: BASIC PHYSICS AND METHODS

Having generalized our earlier solution for the Alfvén wings, we can now apply it to the case of a bounded, non-uniform ionosphere. In order to simplify the problem, we consider the tethered system to be immersed in a uniform geomagnetic field. The system's motion is taken to be in a horizontal plane above the flat, conductive Earth. Its velocity vector is perpendicular to the plane formed by the vertical and the geomagnetic field lines. This corresponds to the situation described in the first part of the preceding section and illustrated in Figure 3.1. We will adhere to the notation of the previous section in the following analysis.

The first significant new feature we introduce to the problem is the presence of boundaries: the one between the ionosphere and the atmosphere and the one between the atmosphere and the Earth. For simplicity, we begin our analysis with the atmospheric cavity considered as a vacuum and the Earth as a perfect conductor. For electromagnetic problems the first approximation is reasonable, and the second approximation greatly simplifies the boundary value problem at the Earth. If the ocean surface is considered, it is justifiable as a first approximation since its main consequence is a small horizontal electric field component at the surface.

A complete, self-consistent solution to the problem of an electrodynamic tethered satellite system operating in the more realistic environment described above is beyond the reach of this analysis. We make the assumption that the tethered system is sufficiently far from the atmospheric boundary (or any steep gradients in plasma parameters) that we need not be concerned with the boundaries' effects on the system.

That is, we assume that the infinite-medium solution previously obtained is a reasonable approximation to the "incident" wave-packet generated by the system operating in the bounded ionosphere. We do not claim to have established criteria by which to judge what "far enough away" means, but our feeling is that the approach can be fruitful if the system is sufficiently far from a boundary that it (including its local Alfvén wing structure) moves into a region previously unoccupied by any part of itself within twice the transit time of an Alfvén wave to the boundary; i.e., if the system has "moved on" before the reflected wave arrives. It should be noted that TSS-1 cannot be expected to satisfy this condition most of the time because of the steep plasma density gradients between its 300 km orbit and the atmospheric cavity. For now we assume a tethered system high in the ionosphere. We restrict ourselves to the steady-state operation of such a system and take the solution of the previous section as the incident Alfvén wave packet. We allow only vertical variations in ionospheric quantities.

The complexity of our problem, even in the simplified form stated above, requires a numerical analysis. There are, however, a number of observations that can be made based on the fundamental physics of the system under consideration. Our approach follows the general outlines of the analyses of ionospheric waves made by P. Greifinger [1972], C. and P. Greifinger [1973], and Rudenko, et al., [1985]. The particularities of our moving source require some modifications to the analysis from the outset, however. In order to utilize the formalism of the above-mentioned authors, we seek an incident wave solution written in terms of plane waves in the horizontal plane, the amplitudes of these wave components being dependent on the vertical co-ordinate, y' in our notation. A number of transformations, which will be defined in de-

tail below, are required to obtain this form for our incident wave-packet. We must also take into account the relationship that exists between the x component of the wave vector and the frequency (as seen in the plasma, i.e. the terrestrial, rest frame) for the steady-state operation of an electrodynamic tethered system: namely, the Döppler relation $\omega = k_x v_x$. This consequence of the constant tether current (which, it should be remembered, is an assumption about the nature of the interaction between the tethered system and the ionosphere) turns out to be of great importance to the electromagnetic field on the Earth's surface, which we are hoping to calculate. At this initial stage of our analysis we restrict ourselves to the Alfvén region $k_x v_x << \Omega_a$, which is consistent with our consideration of systems in the upper regions of the ionosphere.

Following the pattern used to derive expressions (4) and (8) in the preceding section, we obtain the following expressions[*] for the Fourier transformed electric field components

$$E_{x,y} = \frac{8i\omega I}{k_\perp^2 c^2} \delta(\omega - k_x v_x) \frac{\sin\left(\dfrac{k_x L_x}{2}\right)}{k_x L_x} \frac{\sin\left(\dfrac{k_y' L}{2}\right)}{\left(k_z^2 - \varepsilon_\perp\left(\dfrac{\omega}{c}\right)^2\right)} k_{x,y} \tag{16}$$

---

[*] In all that follows we will use the notation $k_y' \equiv k_{y'}$, etc. to represent vector components in the primed system of co-ordinates.

where the $\perp$ subscript refers to components perpendicular to the magnetic field, which lies along the negative z direction.

Thus Maxwell's equations give us

$$B_z = - \frac{c}{\omega}(k_x E_y - k_y E_x) = 0 \qquad (17)$$

Since $E_z = 0$ by assumption, Maxwell's equations further yield

$$B_{y,x} = \pm \frac{k_z c}{\omega} E_{x,y} \qquad (18)$$

These equations represent only the Fourier amplitudes of the field components. The full expressions include the plane wave complex exponential factors $\exp(- i(\omega t - k \cdot x))$.

Our first step in obtaining the desired expressions for the horizontal field components in terms of horizontal plane waves is to carry out the inverse Fourier transform integration over k_z. Since we are considering downward moving waves, which correspond to the negative z direction in our co-ordinate system, we close the contour of integration in the lower half of the complex k_z plane and pick up the contribution of the pole at

$$k_z = - \frac{\omega}{v_A}$$ (19)

We thus arrive at

$$E_{x,y} = \frac{-2Iv_A}{\pi c^2} \int \int \int d\omega \, dk_x \, dk_y \left\{ \exp\left(-i\left[\omega t - k_x x - k_y y + \frac{\omega}{v_A}z\right]\right) \right.$$ (20)

$$\left. \delta(\omega - k_x v_x) \frac{\sin\left(\frac{k_x L_x}{2}\right)}{k_\perp^2 k_x L_x} \sin\left(\frac{k'_y L}{2}\right) k_{x,y} \right\}$$

where k'_y is evaluated with $k_z = - \frac{\omega}{v_A}$.

We now use

$$k_y \, y + k_z z = k'_y \, y' + k'_z z'$$ (21)

and the transformation of variables

$$\int \int \int d\omega \, dk_x \, dk_y = \sin\theta \int \int \int d\omega \, dk_x \, dk'_z$$ (22)

to obtain

$$E_x = \frac{-2Iv_A \sin \theta}{\pi L_x c^2} \int \int \int d\omega \, dk_x \, dk'_z \left\{ \exp\left(-i\left[\omega t - k_x x - k'_y y' - k'_z z'\right]\right) \right.$$

$$\left. \delta(\omega - k_x v_x) \frac{\sin\left(\frac{k_x L_x}{2}\right)}{k_\perp^2} \sin\left(\frac{k'_y L}{2}\right) \right\} \tag{23}$$

$$E_y = \frac{-2Iv_A \sin \theta}{\pi L_x c^2} \int \int \int d\omega \, dk_x \, dk'_z \left\{ \exp\left(-i\left[\omega t - k_x x - k'_y y' - k'_z z'\right]\right) \right.$$

$$\left. \delta(\omega - k_x v_x) \frac{\sin\left(\frac{k_x L_x}{2}\right)}{k_\perp^2 k_x} \sin\left(\frac{k'_y L}{2}\right)\left(k'_y \cos \theta - k'_z \sin \theta\right) \right\} \tag{24}$$

where

$$k'_y = -\frac{\omega}{v_A \sin \theta} - k'_z \cot \theta \tag{25}$$

and

$$k_\perp^2 = k_x^2 + \left(k'_y \cos \theta - k'_z \sin \theta\right)^2 \tag{26}$$

The horizontal wave-vector k lies in the x-z' plane. The
x axis is in the direction of the orbital velocity.
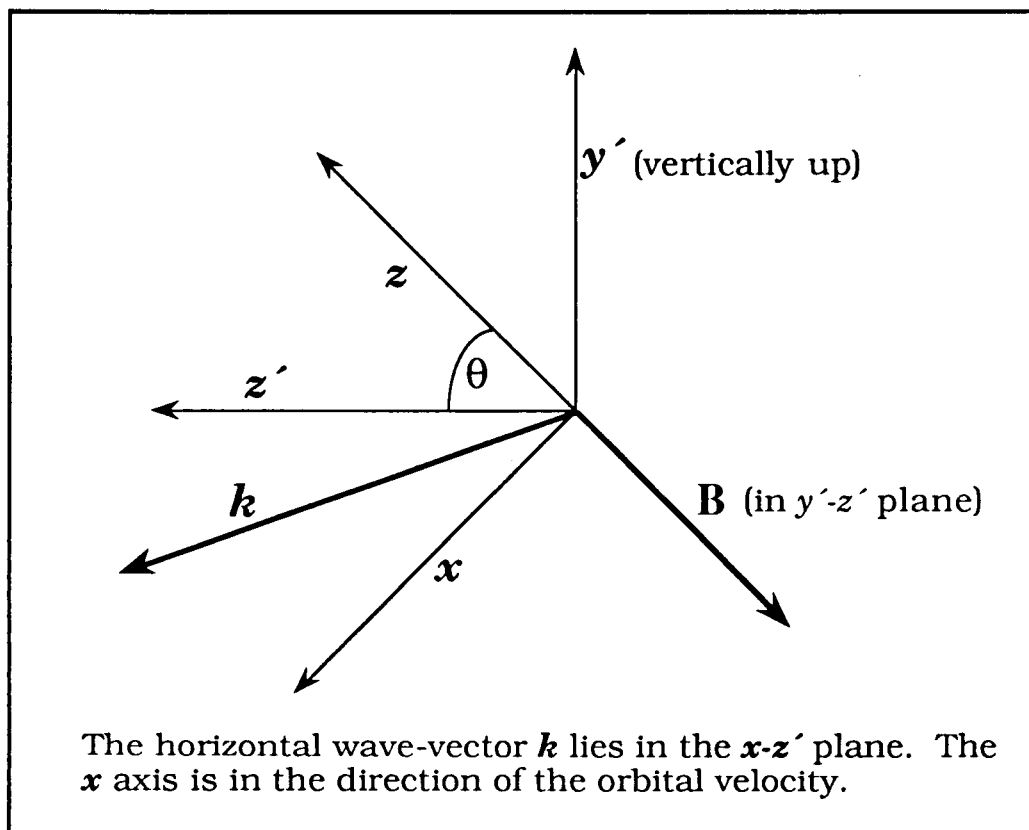
Figure 4.1.   The geometry of the problem

All vectors lie in the horizontal plane. δ is parallel to the horizontal k vector. β is chosen to make a right-handed orthogonal system of $(\delta,\ y',\ \beta)$
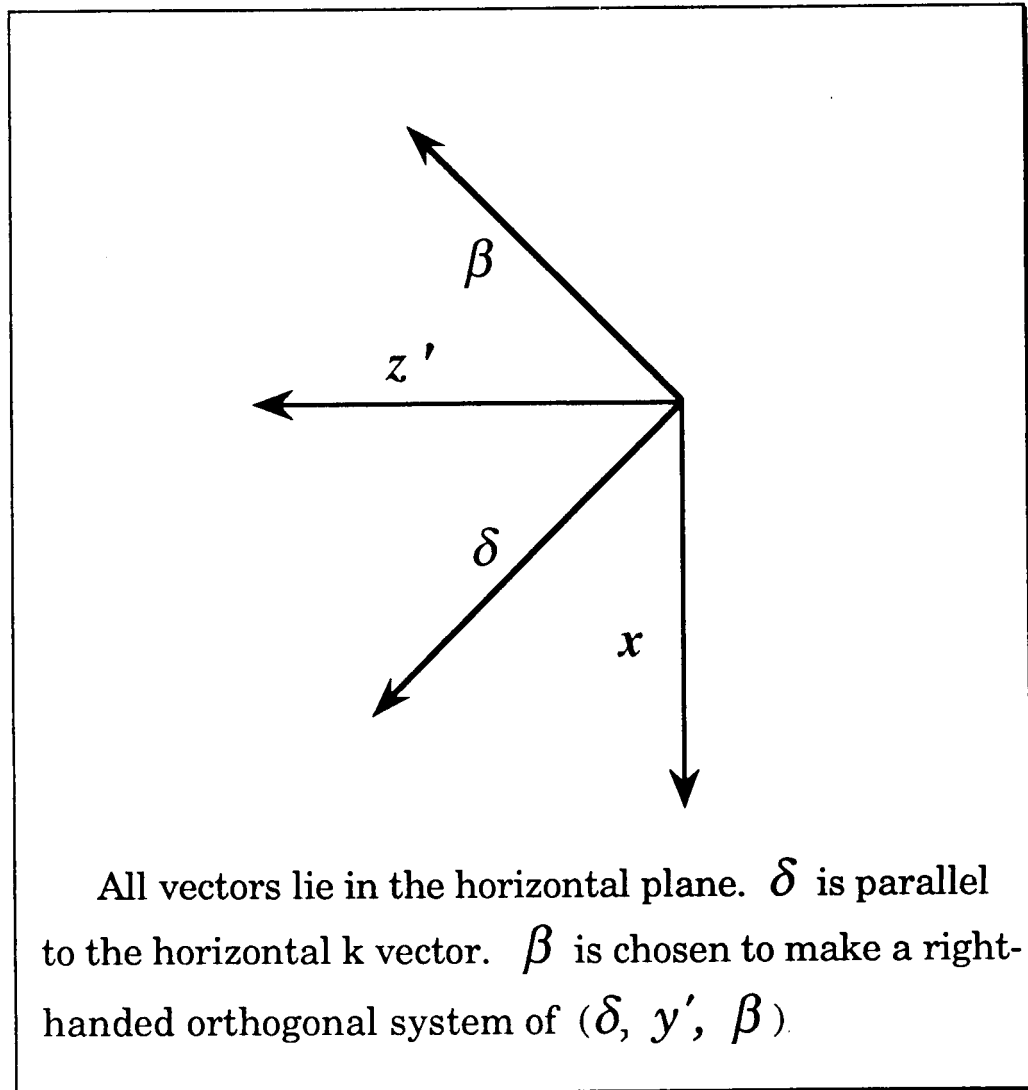
Figure 4.2. The co-ordinate system defined by the horizontal wave vector

Equations (18) and (19) imply

$$B_{x,y} = \pm \frac{c}{v_A} E_{y,x} \tag{27}$$

The horizontal components of the field are now at hand. The x-component is one horizontal component. The other horizontal component of the wave field (the z'-component) is easily obtained utilizing $E_z = B_z = 0$:

$$E'_z = - E_y \sin \theta \tag{28}$$

The corresponding expression holds true for the B field components.

Following the approach of the references mentioned earlier (particularly Rudenko, et al.), we now need to obtain the horizontal wave field components parallel and perpendicular to the horizontal wave vector. Figures 4.1 and 4.2 show the co-ordinates to which we refer. Note that each horizontal wave vector $\left(k_x, k'_z\right)$ defines a different co-ordinate system (δ, β). This implies that we will have to carry out our numerical integration separately for each $\left(k_x, k'_z\right)$ pair. In all that follows the vector k with no subscript refers to the horizontal wave vector of magnitude

$$k = \sqrt{k_x^2 + k_z'^2} \tag{29}$$

In the (δ, β) system the wave electric field components are

$$E_\delta = \frac{\mathbf{E} \cdot \mathbf{k}}{k} \tag{30}$$

$$E_\beta = \hat{\mathbf{y}} \cdot \left(\frac{\mathbf{E} \times \mathbf{k}}{k} \right) \tag{31}$$

The corresponding expressions hold for the components of the $\mathbf{B}$ field.

Having obtained the components of the incident wave packet , we can consider some of the general physical characteristics of the system. The equations to be integrated in the ionosphere will be presented in detail in the next section. We will allow for vertical variations in plasma quantities. These variations include the sharp changes at the boundaries in our problem. Since the only variations in our model are in the vertical direction, the dependence of our incident Alfvén wing wave packet components on the horizontal co-ordintates remains the same throughout and is given by the horizontal plane wave factor. Thus each component of the incident wave packet will arrive at the boundary between the ionosphere and the atmosphere with the same

horizontal wave vector that it had high in the ionosphere. This has important consequences for the solutions in the atmosphere and on the Earth.

The equations for the horizontal field components in the atmospheric cavity are

$$\frac{d^2 E_{\delta, \beta}}{dy'^2} + \left(\frac{\omega^2}{c^2} - k^2\right) E_{\delta, \beta} = 0 \tag{32}$$

$$\frac{d^2 B_{\delta, \beta}}{dy'^2} + \left(\frac{\omega^2}{c^2} - k^2\right) B_{\delta, \beta} = 0 \tag{33}$$

where k, the magnitude of the horizontal wave vector, has the same value as in the ionosphere. Similarly, the frequency is unchanged across the boundary.

The incident wave components contain the factor $\delta(\omega - k_x v_x)$, a consequence of the steady-state operation that we have assumed up until now. An immediate consequence of this is that the factor $\left(\frac{\omega^2}{c^2} - k^2\right)$ in the second term of equations (39) and (39) is always negative, since $|k_x v_x| < |kc|$ always.

This means that the Alfvén wings generated by the steady state operation of an electrodynamic tethered satellite system *will not propagate into the atmospheric cavity*. That is, there is total reflection at the atmosphere's boundary with the ionosphere. Our solution corresponds to a surface wave at the ionospheric boundary.

Taking into account the perfect conductor boundary condition at the Earth's surface, we obtain the solution in the atmospheric cavity

$$E_{\delta, \beta} = E_{\delta, \beta}(y'_b) \frac{\sinh\left(p\left(y' - \left(y'_b - H\right)\right)\right)}{\sinh(pH)} \tag{34}$$

$$B_\beta = \frac{i\omega}{pc} E_\delta(y'_b) \frac{\cosh\left(p\left(y' - \left(y'_b - H\right)\right)\right)}{\sinh(pH)} \tag{35}$$

$$B_\delta = -\frac{ipc}{\omega} E_\beta(y'_b) \frac{\cosh\left(p\left(y' - \left(y'_b - H\right)\right)\right)}{\sinh(pH)} \tag{36}$$

where

$$p = \sqrt{k^2 - \frac{\omega^2}{c^2}} \tag{37}$$

and y'_b and H are the values of y' at the ionospheric boundary and the distance of this boundary from the Earth's surface , respectively.

Equations (35)-(36) show that the ratio of the magnetic field on the Earth's surface to that at the ionospheric boundary is

$$\frac{B_{\delta, \beta}(y'_b - H)}{B_{\delta, \beta}(y'_b)} = (\cosh(pH))^{-1} \tag{38}$$

The height of the ionosphere may be taken to be around 100 km. The consequence of equations (35)-(38) is that the image of the Alfvén wings on the Earth's surface will be much wider than the wings are in the ionosphere, since only the wavepacket components with horizontal wavelengths of hundreds of kilometers will escape severe attenuation. Since such long wavelength components make up only a small fraction of the wavepacket for a reasonably sized tethered system and since the noise level is much higher for the lower regions of the ULF band, we tentatively conclude that the magnetic field image of the Alfvén wings on the Earth's surface will probably be too weak to detect in the case of a steady-current tether, even one with a high current.

Hughes and Southwood [1976] reached similar conclusions about the "shielding" of ionospheric disturbances with short horizontal wavelengths. These authors emphasized the role of Hall currents in the lower part of the ionosphere in reducing the B_β component of the ionospheric waves; but it is obvious from the analysis that the result is quite general since equation (35) is a consequence of Maxwell's equations and the boundary conditions and would hold for different models of the ionospheric conductivity

So far we have not discussed the possible effects of vertical variations in plasma density and ionic composition. Since the Alfvén speed depends directly on

these quantities, their variation changes the effective dielectric constant of the plasma. This has consequences for the waves that can propagate in the ionosphere. The dispersion relation for the anisotropic Alfvén wave is

$$\omega = k_z v_A \qquad (39)$$

The dispersion relation for the fast magnetosonic (isotropic Alfvén) wave is

$$\omega^2 = k_{tot}^2 \, v_A^2 \qquad (40)$$

where k_{tot} is the total wave vector, including horizontal and vertical components. For a given horizontal wave-vector, frequency, and Alfvén speed combination it may be impossible to find a real vertical wave vector component that satisfies the dispersion relation(40). In this case the fast magnetosonic mode is evanescent. This is the case for the steady-current electrodynamic tether, which excites waves satisfying (39), but by virtue of the $\omega = k_x v_x$ condition cannot satisfiy (40) for any real vertical wave vector component. The fast magnetosonic mode has thus been discarded in our calculations of the Alfvén wings. As an aside, we note that this neglect of the fast magnetosonic mode, quite justifiable in the infinite plasma case, where only propagating waves are considered, should probably be re-examined in the bounded plasma case.

We have seen that for a given horizontal k vector and frequency ω, the isotropic wave will propagate or not depending on the Alfvén speed. The Alfvén speed has a minimum value in the F-region of the ionosphere, so an isotropic wave can be con-

fined to the regionaround this minimum—the ionospheric wave guide. Figure 4.3 schematically depicts the ionospheric wave-guide. The Greifinger and Rudenko references discuss the ionospheric wave-guide and note the occurrence of wave-guide resonances. Rudenko, *et al.*. make the point that an Alfvén wave, incident from high in the ionosphere, can couple to the fast magnetosonic wave , through ion-neutral collisions, within the ionospheric wave-guide region for the particular frequency and wave-vector combination.

The ionospheric wave-guide traps electromagnetic energy in a horizontal layer of the ionosphere. Stimulating resonances of the ionospheric wave-guide with an electrodynamic tether would seem to be a possible way of overcoming the difficulties in obtaining a measurable signal on the Earth's surface. It is easy to see that no steady-current electrodynamic tethered system can achieve this in the Earth's ionosphere, however. Since an orbiting steady-current tether cannot stimulate propagating fast magnetosonic waves even in the region of minimum Alfvén speed, it is impossible for Alfvén waves generated by a steady-current tether anywhere in the ionosphere to excite propagating fast magnetosonic waves. *There is no ionospheric wave-guide for steady-current tethers.*

The next phase of our research into the problem of tether-generated electromagnetic waves will focus on the ionospheric wave-guide and its possible excitation by electrodynamic tethered satellite systems with time-varying currents. In the next section we map out the method we plan to use in our numerical investigation of this question.
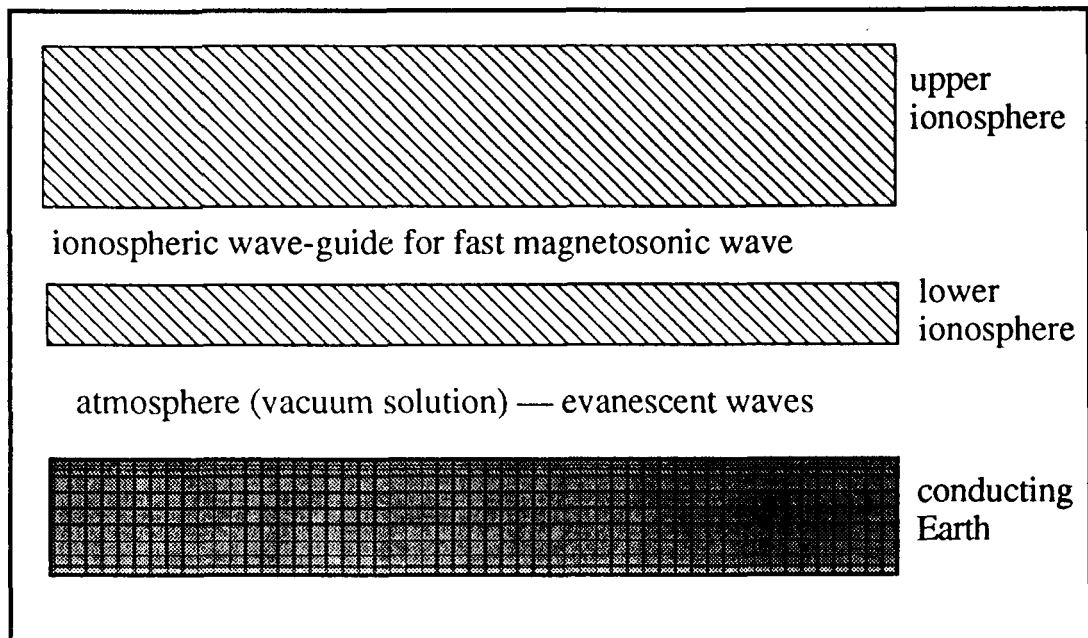
Figure 4.3.   The ionospheric wave-guide and other layers of the medium

5. METHOD FOR INVESTIGATING WAVE-GUIDE EXCITATION

We should state from the outset that our approach is not applicable to all types of tether wave problems. It should be possible to extend the method, however, once it has proven its value. In its present form, the method can be applied to the case where the tethered satellite system is well above the ionospheric wave-guide for the the waves it generates. That is, it applies to a system that directly excites only anisotropic (shear) Alfvén waves. The integration method would thus apply to the case of a steady-current tether; but, as we have already noted, the ionospheric wave-guide concept does not apply to such systems, since there is no region of the ionosphere that will propagate isotropic Alfvén waves that concurrently satisfy the shear Alfvén wave dispersion relation appropriate to a steady-current tether. Thus we would expect the method to have its greatest utility in the case of slowly-varying tether currents with frequency components such that coupling to ionospheric wave-guide modes occurs.

It should also be noted that we are talking only about variations in the tether current sufficiently slow that all of the previous work on steady-current tether wave generation applies with only slight modification. This means that the tether current distribution can still be considered as independent of the vertical co-ordinate along the tether's length. The tether is not functioning as an antenna in the normal sense of the word in this case, any more than it does in the steady-current case. It is still a source of varying current to the ionospheric transmission line, a concept that we have emphasized in our previous analysis. The ionospheric waves generated by the tether are due to the charge it injects into the ionosphere at each end of the system, rather than to direct radiation from the tether.

We assume a tether current distribution that is just expression (1) multiplied by $\cos(\omega_0 t)$, where ω_0 is the oscillation frequency of the tether current. How this oscillation is achieved need not concern us too much at this stage. Let us suppose that the tethered system is equipped with a suitable power supply to enable it to reverse the current. Any time variation can be broken into its Fourier components, so the choice is not restrictive, except that we are explicitly excluding spatial variations in the tether current along its length, which implicitly limits the range of frequencies we can consider.

Expressions (23) and (24), which define the incident wave packet, are modified only by the replacement of the delta function $\delta(\omega - k_x v_x)$ by

$$\frac{(\delta(\omega + \omega_0 - k_x v_x) + \delta(\omega - \omega_0 - k_x v_x))}{2} \tag{41}$$

Having derived the incident Alfvén wave-packet, we now turn our attention to the numerical methods we propose to use for solving the problem. We are following the method outlined in Rudenko, *et al.*, However, our notation differs in some respects from that used in the Rudenko reference. In addition there are a few serious typographical errors in that paper. For these reasons, and to make this report stand alone, we will outline the method here.

The incident wave solution we have obtained applies to a region where the ion-neutral collision frequency is negligible and the Alfvén speed is constant. Anticipating the variations in plasma quantities that occur lower in the ionosphere, we express Maxwell's equations in the following compact way :

$$-i\frac{d\,F}{dy'} = G\,F \tag{42}$$

where we define F as the four component vector

$$F = (\,E_\delta,\ E_\beta\ H_\delta,\ H_\beta\,) \tag{43}$$

with the third and fourth components given by

$$H_\delta = -\left(\frac{v_0\ \overline{\omega}}{c}\right)B_\beta \tag{44}$$

$$H_\beta = \left(\frac{v_0\ \overline{\omega}}{c}\right)B_\delta \tag{45}$$

For our numerical work we use dimensionless quantities. The dimensionless frequency is defined by

$$\overline{\omega} = \frac{\omega\lambda}{v_0} \tag{46}$$

where λ is a linear scaling factor and v_0 is the Alfvén speed in the region in which the wave-packets originate. The variable $\bar{y}'$ is just the vertical spatial co-ordinate in units of λ.

In expression (42) G represents the 4×4 matrix

$$G = \begin{pmatrix} g_1 & g_2 \\ g_3 & g_4 \end{pmatrix} \qquad (47)$$

defined by the 2×2 submatrices

$$g_1 = \begin{pmatrix} -\bar{k}_z \cot\theta & -\bar{k}_x \cot\theta \\ 0 & 0 \end{pmatrix} \qquad (48)$$

$$g_2 = \begin{pmatrix} 1 & 0 \\ 0 & 1 \end{pmatrix} \qquad (49)$$

$$g_3 = \begin{pmatrix} \dfrac{\bar{\omega}^2}{\bar{v}^2} \mu_1 \left(\dfrac{\bar{k}^2 - \bar{k}_x^2 \cos^2\theta}{\bar{k}^2 \sin^2\theta} \right) & \dfrac{\bar{\omega}^2}{\bar{v}^2} \left(\dfrac{\mu_1 \bar{k}_x \bar{k}_z \cot^2\theta}{\bar{k}^2} - \dfrac{\mu_2}{\sin\theta} \right) \\[3ex] \dfrac{\bar{\omega}^2}{\bar{v}^2} \left(\dfrac{\mu_1 \bar{k}_x \bar{k}_z \cot^2\theta}{\bar{k}^2} + \dfrac{\mu_2}{\sin\theta} \right) & \dfrac{\bar{\omega}^2}{\bar{v}^2} \mu_1 \left(\dfrac{\bar{k}^2 - \bar{k}_x^2 \cos^2\theta}{\bar{k}^2 \sin^2\theta} \right) - \bar{k}^2 \end{pmatrix} \qquad (50)$$

$$g_4 = \begin{pmatrix} -\bar{k}_z \cot\theta & 0 \\ -\bar{k}_x \cot\theta & 0 \end{pmatrix} \qquad (51)$$

In the expressions above $\bar{k}_z$ and $\bar{k}_x$ refer to the dimensionless horizontal wave-vector components defined by the scaling factor λ. The normalized Alfvén speed $\bar{v}$ is defined by $\dfrac{v_A}{v_0}$.

The quantities

$$\mu_1 = \frac{\left(1 + i\,\dfrac{v_i}{\omega}\right)}{\left(1 + \left[\dfrac{(v_i - i\,\omega)}{\Omega_{ci}}\right]^2\right)} \qquad (52)$$

and

$$\mu_2 = i\left(\frac{\omega}{\Omega_{ci}}\right)\left[1 + i\,\frac{v_i}{\omega}\right]\mu_1 \qquad (53)$$

along with the Alfvén speed, express the dielectric properties of the ionospheric medium. Here v_i and Ω_{ci} are the ion-neutral collision frequency and the ion cyclotron frequency, respectively. The Alfvén speed, v_i, and Ω_{ci} all vary with altitude in our model.

For the frequency range and horizontal wave-vectors to which we are limiting our analysis, there are four well-defined independent solutions to equation (42) in the upper ionosphere: two shear Alfvén solutions, corresponding to positive and negative vertical wave-vector components, and two isotropic Alfvén solutions, one that grows exponentially with increasing y' and another that falls off exponentially with increasing y'. The shear Alfvén solution with negative vertical wave-vector component corresponds to our incident wave. The amplitude for each horizontal wave-vector component is given by (23)-(27), as modified by the substitution of (41) as specified above. The upward traveling shear Alfvén solution then corresponds to a reflected wave. Of the two isotropic Alfvén wave solutions, only the upwardly decreasing solution makes physical sense. This corresponds to leakage of the ducted fast magnetosonic wave from the ionospheric wave-guide. Thus we are left with three physically meaningful solutions to equation (42) at "infinity" (which is the short-hand expression we will use to indicate the location of our tethered system, high in the ionosphere).

While we know the amplitude of the incident wave-packet solution at infinity, the amplitudes of the other two solutions are unknown and must be the result of complex interactions in the lower ionosphere. It turns out that knowledge of the functional form of these solutions at infinity, combined with the boundary conditions at the ionosphere/atmosphere interface and our knowledge of the functional form of the solutions in the atmospheric cavity (Equations (34)-(37)) will suffice to determine a solution at the boundary between the atmosphere and ionosphere and, hence, on the Earth's surface.

Let us now sketch the means by which this can be accomplished. First we introduce the admittance matrices, which are variations of those defined by Budden in the "Bible" of ionospheric wave physics *The Propagation of Radio Waves* [1985]. We define the admittance matrix $A^{(i,j)}(\overline{\omega}, \overline{k}, \overline{y}')$ as the 2×2 matrix that satisfies the equation

$$\begin{pmatrix} \alpha F_3^i + \beta F_3^j \\ \alpha F_4^i + \beta F_4^j \end{pmatrix} = A^{(i,j)}(\overline{\omega}, \overline{k}, \overline{y}') \begin{pmatrix} \alpha F_1^i + \beta F_1^j \\ \alpha F_2^i + \beta F_2^j \end{pmatrix} \tag{59}$$

where F^i and F^j are two solutions of (42) and α and β are two arbitrary complex constants. In other words, the admittance matrix transforms a linear combination of the electric field components of the two independent solutions into the same linear combination of the corresponding magnetic field components, as defined by equations (43)-(45).

This is equivalent to

$$\begin{pmatrix} F_3^i & F_3^j \\ F_4^i & F_4^j \end{pmatrix} = A^{(i,j)}(\overline{\omega}, \overline{k}, \overline{y}') \begin{pmatrix} F_1^i & F_1^j \\ F_2^i & F_2^j \end{pmatrix} \tag{60}$$

It is straightforward to obtain from (42) and (60) the following differential equation for an admittance matrix A defined as in (59) and (60):

$$- i \frac{dA}{dy'} = - A A - A g_1 + g_4 A + g_3 \qquad (61)$$

where the g_i are the matrices defined in (48)-(51).

The admittance matrices contain the ratios of electromagnetic field components rather than their absolute values. This has an important advantage for numerical integrations down through the ionosphere, since it avoids the problem of numerical swamping brought on by the exponential growth of an initially small mix of the solution that grows as the altitude decreases.

Since we know the functional form of the solutions at infinity, we can construct the admittance matrices at infinity in the following way:

$$\overset{(i,j)}{A}(\omega, k) = \begin{pmatrix} X_3^i & X_3^j \\ X_4^i & X_4^j \end{pmatrix} \begin{pmatrix} X_1^i & X_1^j \\ X_2^i & X_2^j \end{pmatrix}^{-1} \qquad (62)$$

where the X^i are the known functional forms of the F^i solutions at infinity. These can then be taken as the initial values for numerical integration down to the boundary with the atmosphere.

A^b, the boundary matrix at the atmosphere/ionosphere boundary is defined by

$$\begin{pmatrix} F_3(\bar{y}'_b) \\ F_4(\bar{y}'_b) \end{pmatrix} = A^b \begin{pmatrix} F_1(\bar{y}'_b) \\ F_2(\bar{y}'_b) \end{pmatrix} \tag{63}$$

where the F corresponds to the total solution at the boundary, including the contributions from the reflected and ducted waves, as well as the incident wave.

For the case of a perfectly conducting Earth this corresponds to

$$A^b = i\lambda \coth\,(\,pH\,) \begin{pmatrix} \left(\dfrac{\omega^2}{c^2 p}\right) & 0 \\ 0 & -p \end{pmatrix} \tag{64}$$

The solution at the boundary may be written as

$$F(\bar{y}'_b) = B_1 F^1(\bar{y}'_b) + B_2 F^2(\bar{y}'_b) + B_3 F^3(\bar{y}'_b) \tag{65}$$

where F^1 and F^2 denote the reflected and incident shear Alfvén solutions, respectively, and F^3 denotes the ducted wave solution, with the B_i complex constants. The coefficient B_2 is known from the incident shear Alfvén solution at infinity.

An obvious consequence of the definition of the admittance matrices (59) is that

$$\left(A^{(i,j)}(\overline{\omega}, \overline{k}, \overline{y}') - A^{(k,j)}(\overline{\omega}, \overline{k}, \overline{y}') \right) \begin{pmatrix} F_1^j \\ F_2^j \end{pmatrix} = 0 \qquad (66)$$

for $i \neq k$.

We can utilize expressions (59), (63), (65), and (66) to obtain the following equation, which is true on the boundary of the ionosphere and the atmosphere:

$$\left(A^b(\overline{\omega}, \overline{k}) - A^{(1,3)}(\overline{\omega}, \overline{k}, \overline{y}_b') \right) \begin{pmatrix} F_1 \\ F_2 \end{pmatrix} = \qquad (67)$$

$$\left(A^{(2,3)}(\overline{\omega}, \overline{k}, \overline{y}_b') - A^{(1,3)}(\overline{\omega}, \overline{k}, \overline{y}_b') \right) B_2 \begin{pmatrix} F_1^{(2)} \\ F_2^{(2)} \end{pmatrix}$$

This expression, which relates the electric field components of the total solution (65) on the boundary to the electric field components of the incident wave solution on the boundary by means of the admittance and boundary matrices, is the basis for

our numerical method. We can invert the matrix $\left(A^{b}(\overline{\omega}, \pmb{k}) - A^{(1,3)}(\overline{\omega}, \pmb{k}, \overline{y}'_{b}) \right)$ on the left hand side of (67) to obtain the electric field components on the boundary. Then the boundary matrix A^{b} yields the magnetic field components on the boundary. The atmospheric cavity solution (35)-(36) yields the magnetic field on the Earth's surface and anywhere in the atmosphere. The required admittance matrices and the incident wave solution on the boundary are to be obtained by means of numerical integration of the equations (61) and (42).

All of the analysis outlined in the preceding paragraphs must be carried out for each horizontal wave vector component. The complete solution on the Earth's surface is obtained by summing over all these solutions to obtain the inverse Fourier transform. A sort of flow chart of the method is shown in Figure 5.1.

This is the scheme we propose to carry out to obtain the first approximation to the electromagnetic field on the Earth's surface due to an orbiting electrodynamic tethered satellite system with a slowly varying current. It requires a model for the ionosphere that includes vertical profiles of the plasma density, the effective ion mass, and the ion-neutral collision density. Other assumptions of the theory are discussed in the concluding chapter. We have begun software development to carry out the program of numerical analysis.

STARTING POINT: Electrodynamic Tether serves as a steady-state or slowly varying current source in the ionosphere (considered as an infinite Alfvén medium)

Fourier Transform ⟶

⟵ Maxwell's Equations

Alfvén wave-packet in k space serves as incident wave solution (Alfvén wings)

Transform to horizontal ⟶ and vertical k components

⟵ Transform each field component to (δ, β) system.

Alfvén wave-packet now in form we can integrate down to atmospheric boundary

Integrate incident wave-packet component ⟶

⟵ Obtain and integrate admittance matrices for given k

Now have A matrices and F vector at atmospheric boundary

⟵ Apply boundary matrix and solve for B

Now have B on the boundary for a given horizontal k component

⟵ Apply vacuum solution for atmosphere

B on the Earth's surface for a given horizontal k component

Transform from the (δ, β) system to the (x, z') system. ⟶

B on the Earth's surface in the (x, z') system for a given horizontal k

⟵ Repeat the whole process for all k and sum the k components
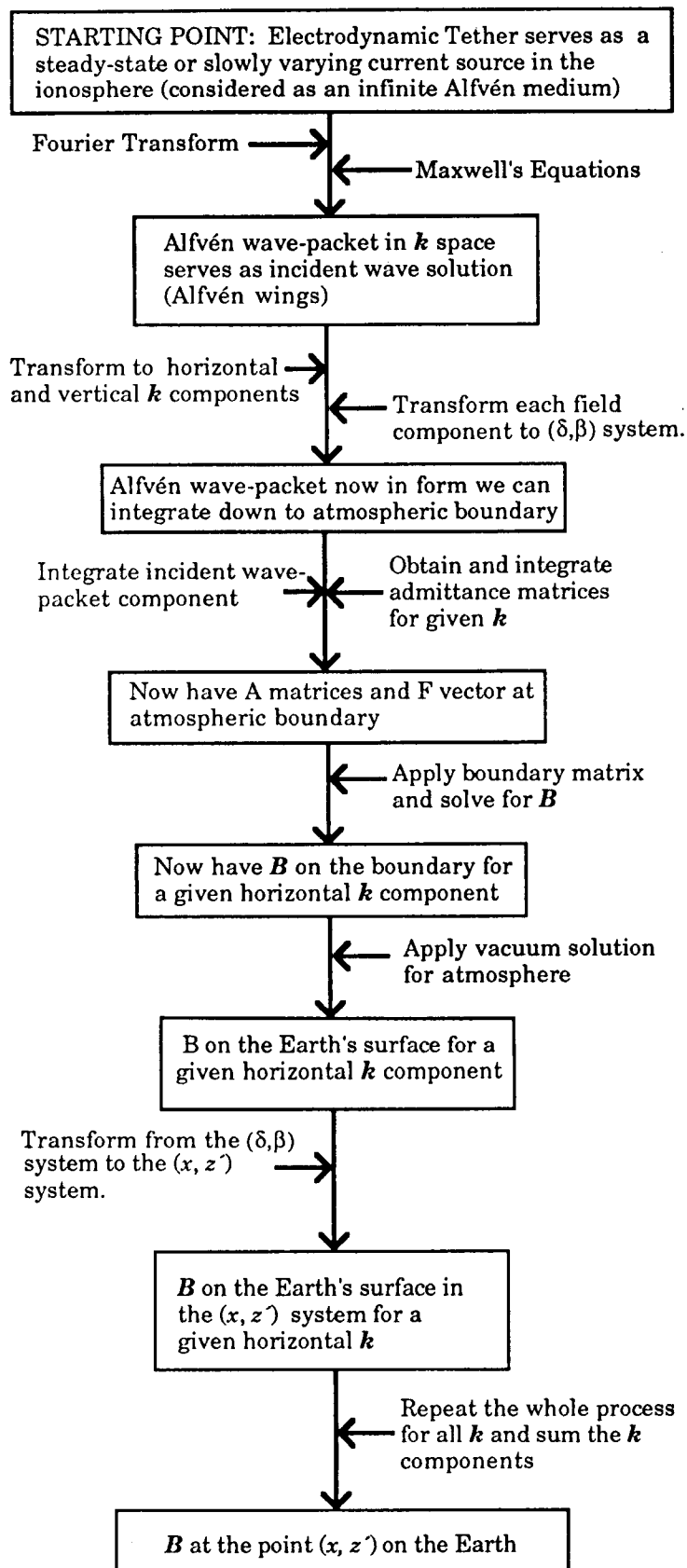
B at the point (x, z') on the Earth

Figure 5.1.   Flow chart of the complete computation

6.   CONCLUSIONS AND PERSPECTIVE

During the course of this work we have re-examined our previous analysis of ionospheric wave excitation.by electrodynamic tethers in an infinite medium. Our rebuttal to the criticisms made by Dobrowolny and his co-workers is contained in the Appendix. We remain convinced that our analysis was sound, and it appears that most investigators in the field concur. We note that Barnett and Olbert of M.I.T. have acknowledged that our analysis, as contained in the *JGR* paper, was correct in pointing out that their orbiting wire model of the tether lacked physical sense and led to a gross overestimation of the contribution of the lower hybrid frequency band to the tether wave impedance.

We have generalized the analysis to the case where the geomagnetic field lines make an arbitrary angle with the vertical. The generalized solution thus obtained has then served as the starting point for a first approximation to the much more difficult problem of tether-generated Alfvén wave packet propagation through a non-uniform ionosphere bounded by the atmosphere, which is in turn bounded below by a conducting Earth.

We have discussed the physics of the ionospheric wave-guide for fast magnetosonic waves and noted the possible importance of the excitation of ionospheric wave-guide modes coupled to the incident shear Alfvén waves generated by the tethered system. A steady-current electrodynamic tether will not excite the ionospheric wave-guide, however, as we demonstrate in Section 4.

We have shown that it is possible to gain considerable insight into the physics of an electrodynamic tether in a bounded ionosphere without solving the complete

problem. In addition to the result stated in the previous paragraph, it was also possible to show that the Alfvén wings generated by a steady-current tether are completely reflected at the boundary of the ionosphere with the atmosphere. Thus there is no direct propagation of the waves into the atmosphere, only a leakage of the associated field. On the Earth's surface only wave components with horizontal wave-lengths in the 100 km and greater range would have the same strength as at the ionospheric boundary . Thus the image of the Alfvén wings on the Earth's surface would be much wider than in the ionosphere. The signal strength would probably be too weak to detect, even for high current values.

Thus the problem of time-varying tether currents assumes even greater importance from the standpoint of the signal reaching the Earth. We have made the initial steps in this analysis, carrying the generalization one step further to consider the case of slowly varying tether currents. We have presented in some detail a scheme for obtaining the magnetic field on the Earth's surface for an electrodynamic tethered satellite system with a varying current in orbit above the peak in ionospheric electron density, i.e., above the center of the ionospheric wave-guide. This method, which involves the numerical integration of the initial Alfvén wave-packet and Budden admittance matrices down through the ionosphere, will be applied in our ongoing work on this problem.

It is always good to keep in mind the limitations and assumptions of a theory. The ionospheric plasma is considered to be a linear, dielectric medium. As in previous analyses, we have assumed that the plasma temperature is not important to the waves under consideration, though we have included ion-neutral collisions in our new model

for the dielectric tensor. Based on previous experience, we have simplified the problem by considering only wave components satisfying the magnetohydrodynamic criterion. Vertical variations in plasma density, ion content, and collision frequency are allowed; but horizontal variations, which could be important in practice, are not included. The Earth is flat, the magnetic field uniform. Furthermore, the incident wave-packet has been taken from the infinite medium solution. All of these assumptions could eliminate effects that will turn out to be important. The extension of the analysis to higher frequency tether current variations is clearly a necessary step, but one that will require greater care than the analyses we have seen so far, since determining the current distribution within the tether becomes crucial and requires a self-consistent solution to the problem of the interaction between the tether and the ionosphere.

While acknowledging that much work remains to be done, we feel that the work reported here represents an advance in our understanding of the problem of electromagnetic wave generation and propagation from a tethered satellite system and points the way to further progress.

REFERENCES:

Barnett, A., and S. Olbert, Radiation of plasma waves by a conducting body moving through a magnetized plasma, *J. Geophys. Res.*, 91, 10, 117, 1986.

Belcastro, V., P. Veltri, and M. Dobrowolny, Radiation from long conducting tethers moving in the near earth environment, *Nuovo Cimento C*, 5, 537, 1982.

Budden, K.G., The propagation of radio waves: The theory of radio waves of low power in the ionosphere and magnetosphere, Cambridge Univ. Press, 1985.

Dobrowolny, M., and P. Veltri, MHD power radiated by a large conductor in motion through a magnetoplasma, *Nuovo Cimento Soc. Ital. Fis. C*, 9, 27, 1986.

Drell, S.P., H.M. Foley, and M.A. Ruderman, Drag and propulsion of large satellites in the ionosphere: An Alfvén engine in space, *J. Geophys. Res.*, 70, 3131, 1965.

Estes, R.D. Alfvén waves from an electrodynamic tethered satellite system, *J. Geophys. Res.*, 93, 945, 1988.

Greifinger, P., Micropulsations from a finite source, *J. Geophys. Res.*, 77, 2392, 1972.

Greifinger, C. and P. Greifinger, Wave guide propagation of micropulsations out of the plane of the geomagnetic meridian, *J. Geophys. Res.*, 78, 4611, 1973.

Hughes, W.J. and D.J. Southwood. The Screening of Micropulsation Signals by the Atmosphere and Ionosphere *J. Geophys. Res.*, 81, 3234, 1978.

Rasmussen, C.E., P.M. Banks, and K.J. Harker, The excitation of plasma waves by a current source moving in a magnetized plasma: The MHD approximation, *J. Geophys. Res.*, 90, 505, 1985.

Rudenko, G.V., S.M. Churilov, and I.G. Shukhman, Excitation of the ionospheric waveguide by a localized packet of Alfvén waves, *Planet. Space Sci.*, 33, 1103, 1985.

APPENDIX: An Examination of the Dobrowolny/Veltri Results and
Criticism

In this appendix we will consider in detail the analysis of Dobrowolny and Veltri, since Dobrowolny and his co-workers have continued to maintain that it alone has found the correct solution to the problem of tether wave generation.

We want to make clear that as regards their criticism of our results we will be summarizing verbal remarks Dobrowolny and his colleague Iess have made rather than referring to anything they have written. We believe we have understood their criticisms and will attempt to make a fair presentation of them, while stating from the outset that their arguments have not convinced us. We have in fact rederived our results using their formulation of the problem.

First let us consider their original analysis (as presented in the Nuovo Cimento article by Dobrowolny and Veltri) and compare it with the SAO analysis. Dobrowolny and Veltri use a long orbiting cylinder with square cross-section to model the tethered system. Since D, the tether's transverse dimension, is stated to be on the order of 1 mm, it is clear that this is just another variation of the orbiting wire model, the inadequacy of which we have previously demonstrated. However, the authors do not deal at all with the issue of radiation in other frequency bands raised by Barrett and Olbert. Following a different approach from that of the SAO study, they begin by writing down the most general, all-inclusive formula for the power radiated by a current distribution in a plasma

(equations (9)-(12) in the original):

$$P = \lim_{T \to \infty} \frac{1}{2\pi^2 T} \int d^3k \int \frac{d\omega}{\omega} \lambda_{ss} \; (\vec{k}, \omega) \left| J_j^{(e)*}(\vec{k}, \omega) e_j(\vec{k}, \omega) \right|^2 \delta(\Lambda) \quad (A.1)$$

where

$$\lambda_{ss} = Tr\lambda_{ij} \quad (A.2)$$

and λ_{ij} is the co-factor of the plasma tensor Λ_{ij} defined by

$$\Lambda_{ij} = n^2 \left(\frac{k_i k_j}{k^2} + \delta_{ij} \right) + \epsilon_{ij}(\vec{k}, \omega) \quad (A.3)$$

using standard notation. Finally $\Lambda = det \; \Lambda_{ij}$, and e_j is the polarization vector defined by

$$e_i = \frac{\lambda_{ij} a_j}{\left(\lambda_{ss} a_i^* \lambda_{ij} a_j \right)^{\frac{1}{2}}} \quad (A.4)$$

in terms of an "arbitrary complex vector a." $\vec{J}^{(e)}$ is the external current, which we have denoted by $\vec{j}$. Neither at this point nor at any later point do the authors ever specify the form of ϵ_{ij}. They maintain a high level of abstraction. The meaning of the polarization vector seems particularly obscure to us in this context.

For formula (A.1) the authors refer to *Plasma Astrophysics: Nonthermal Processes in Diffuse Magnetized Plasmas*, Volume 1 by D.B. Melrose. In fact the expression does not appear precisely this way in the reference. What Melrose writes is (equation (3.8) p. 65)

$$P = \frac{-\lim}{T \to \infty} \frac{1}{T} \int \frac{d\omega}{2\pi} \int \frac{d^3k}{(2\pi)^3} \left[\vec{J}^{(e)*}(\vec{k}, \omega) \cdot \vec{E}(\vec{k}, \omega) \right] \qquad (A.5)$$

where we have slightly altered the notation to be consistent with Dobrowolny et al. The integrand in Melrose is the dot product of the Fourier transform of the wave electric field vector and the complex conjugate of the Fourier transform of the external current density, which is the tether current in our case.

Before continuing with our discussion of the analysis of Dobrowolny, et al. let us apply this equation, i.e. the equation as it actually appears in Melrose, to the SAO results.

We have already seen that the contribution of the j_z component to the radiated power is small, so we consider the contribution of $j_y{}^* E_y$. Referring to the previous SAO results, we obtain

$$j_y^* E_y \;=\; \frac{4\pi i\omega}{k_\perp^2 c^2}\; \frac{\vec{k}\cdot\vec{j}}{k_z^2 - \omega^2\epsilon_\perp/c^2}\; k_y j_y^*$$

$$=\; \frac{8I^2 i\omega}{\pi c^2}\, \frac{\big[\delta(\omega - k_x v_x)\big]^2 \sin^2\!\big(k_y L/2\big)\sin\!\big(k_z L_z/2\big)}{k_\perp^2\big(k_z^2 - \omega^2\epsilon_\perp/c^2\big)k_z L_z} \qquad (A.6)$$

Using equation (2.12) (p. 27) of Melrose we can make the substitution

$$\big[\delta(\omega - k_x v_x)\big]^2 \;=\; \lim_{T\to\infty}\, \frac{T}{2\pi}\, \delta(\omega - k_x v_x) \qquad (A.7)$$

Then we obtain the expression for the power going into waves

$$P \;=\; -\,\frac{4I^2 i}{L_z \pi^2 c^2}\, \int d\omega\, d^3k\; \frac{\omega\;\delta(\omega - k_x v_x)\sin^2(k_y L/2)\sin(k_z L_z/2)}{k_\perp^2\cdot\big(k_z^2 - \omega^2\epsilon_\perp/c^2\big)\,k_x} \qquad (A.8)$$

where factors of 2π have disappeared because we use a different convention from Melrose's in defining the Fourier transform. Performing the integration over ω and k_z exactly as before, we get

$$P \;=\; \frac{4I^2 v_A}{\pi L_z c^2}\int_{-K_O}^{K_O} dk_z \int_{-\infty}^{\infty} dk_y\; \frac{\sin^2(k_y L/2)\sin(k_z L_z/2)}{k_\perp^2 k_z}\, \sqrt{1 - \left(\frac{k_z v_x}{\Omega_{ci}}\right)^2} \qquad (A.9)$$

Utilizing the formula

$$\int \frac{\sin^2 ax}{x^2 + \beta^2} \, dx = \frac{\pi}{4\beta} \left(1 - e^{-2a\beta}\right)$$

$$\left(a > 0, \ Re\beta > 0\right) \qquad (A.10)$$

found in Gradshteyn and Ryzhik's tables (p. 447), we finally obtain

$$P = \frac{I^2 v_A}{L_x c^2} \int_0^{K_0} dk_z \left(1 - e^{-k_x L}\right) \frac{\sin(k_z L_z/2)}{k_z^2} \sqrt{1 - \left(\frac{k_z v_z}{\Omega_{ci}}\right)^2} \qquad (A.11)$$

Dividing by I^2 to obtain the impedance Z_A, we find we have arrived at an expression *identical* to the one derived previously in the SAO study. This exercise has demonstrated that by starting from the same point as Dobrowolny et al. we still arrive at the same result as previously. Since expression (A.5) is completely general, this had to be, assuming we had made no errors.

The purpose of this exercise has been twofold: first to point out that if there are errors in the SAO analysis they must have occurred in the derivation of the expression for E_k. Since this derivation is easily followed, it should be possible to discover any errors made there. The point that follows from this is that we should be doubly careful in evaluating the analysis of Dobrowolny et al. which supposedly uses the same starting point.

The SAO analysis made use of the $E_z = 0$ approximation to good purpose. When this is not done, a great deal of unnecessary apparent complexity remains,

with a concurrent increase in the probability that errors in calculations or physical reasoning will occur.

Let us turn our attention to equation (A.1), the starting point for the analysis of Dobrowolny and Veltri. We have already mentioned that it is itself a derived expression not found explicitly in the Melrose reference. Although the authors have not demonstrated the intermediate steps, we can attempt to reconstruct their chain of reasoning.

Melrose gives the general equation ((3.16), p. 67)

$$E_i(\vec{k}, \omega) = \frac{-4\pi i}{\omega} \frac{\lambda_{ij}(\vec{k}, \omega)}{\Lambda(\vec{k}, \omega)} J_j^{(e)}(\vec{k}, \omega) \tag{A.12}$$

This follows from the definitions and the basic wave equation.

Inserting this into equation (A.5) gives

$$P = \frac{-\lim}{T \to \infty} \frac{4\pi i}{T} \int \frac{d\omega}{2\pi\omega} \int \frac{d^3k}{(2\pi)^3} \frac{J_i^{(e)} \lambda_{ij} J_j^{(e)*}}{\Lambda} \tag{A.13}$$

Now for a given mode σ, Melrose defines the polarization vector e_i^σ in the way Dobrowolny and Veltri seem to be doing for all modes, inclusively, in expression (A.4). We have not examined this issue thoroughly, but it is not immediately

obvious to us that this extension makes sense, i.e. that a single arbitrary complex vector $\vec{a}$ would yield physically meaningful results for all modes. Granting this point (They never say what $\vec{a}$ they use.), we then obtain

$$\lambda_{ij} = \lambda_{ss} \, e_i e_j^* \qquad (A.14)$$

which leads to

$$P = \mathop{-\lim}_{T \to \infty} \frac{i}{4\pi^3 T} \int \frac{d\omega}{\omega} \int d^3k \, \frac{\lambda_{ss}}{\Lambda} \, | \, \vec{J}^{(e)*} \cdot \vec{e} \, |^2 \qquad (A.15)$$

This becomes identical with equation (A.1) if we make the substitution

$$\frac{1}{\Lambda(\vec{k},\omega)} = 2\pi i \; \delta\Big(\Lambda(\vec{k},\omega) \Big) \qquad (A.16)$$

At this point, the meaning of $\delta(\Lambda)$ is somewhat ambiguous. Although the authors present the next step in their results without any explanation beyond a characterization of the intermediate calculations as "lengthy", we gather from the factor $| \, \partial\Lambda/\partial\omega \, |^{-1}$ appearing in their result that they are taking the $\delta(\Lambda)$ to mean that Λ is a function of ω, which depends parametrically on $\vec{k}$ insofar as the integration over ω is concerned. Thus the integration gives a sum of terms from the poles of Λ^{-1} (i.e. the zeros of Λ). These poles would correspond to the

solutions of the dispersion relation $\Lambda(\omega, k) = 0$.   Therefore

$$\delta(\Lambda) \;=\; \sum_{\sigma} \quad \delta\Big(\omega - \omega_\sigma(k)\Big) \Big/ \left| \frac{\partial \Lambda}{\partial \omega} \right|_{\omega = \omega_\sigma(k)}$$

where the sum is over the different wave modes.

Since they were only going to consider Alfvén waves, the authors could have saved themselves a lot of computational labor by continuing to follow the analysis presented in Melrose's book.   On page 56 of that work we find that following results

$$\vec{e}^A \;=\; \frac{\vec{k}_\perp}{k_\perp} \tag{A.17}$$

$$\frac{\lambda_{ss}^A(\vec{k})}{\big[\, \omega\, \partial\Lambda \,/\, \partial\omega\, \Lambda \,\big]_{\omega = \omega_A}} \;=\; \frac{V_A{}^2}{2c^2} \tag{A.18}$$

where $\vec{e}^A$ is the Alfvén wave polarization vector.   (Refer to page 36 for the relevant coordinate axes.)

Equation (A.15) thus becomes

$$P_A = \lim_{T \to \infty} \frac{1}{2\pi^2 T} \int d^3k \int_{-\omega_o}^{\omega_o} d\omega \; \frac{\lambda_{ss}}{\left(\omega \, \partial \Lambda / \partial \omega \right)_{\omega = \omega_A}} \; \delta\left(\omega - \omega_A(\vec{k}) \right) \; \frac{J_y^{(e)2} k_y^{\,2}}{k_\perp^{\,2}} \quad (A.19)$$

$$= \lim_{T \to \infty} \frac{V_A^{\,2}}{4\pi^2 T c^2} \int d^3k \int_{-\omega_o}^{\omega_o} d\omega \; \delta\left(\omega - \omega_A(\vec{k}) \right) \; \frac{J_y^{(e)2} \; k_y^{\,2}}{k_\perp^{\,2}} \qquad (A.20)$$

where ω_o is a cut-off frequency such that $\omega_o \ll \Omega_{ci}$.

Continuing in much that same way as in the calculation immediately preceding this one and using the Dobrowolny/Veltri expression for $J^{(e)}$, we obtain

$$P_A = \frac{2I_o^{\,2} V_A}{\pi c^2} \int_{-K_o}^{K_o} dk_z \int \frac{dk_y}{k_\perp^{\,2}} \frac{\sin^2(k_y L/2)\sin^2(k_z V_o D/2 V_A)}{(k_z V_o D/2 V_A)^2 (k_z D/2)^2} \; \sin^2\!\left(\frac{k_z D}{2} \right) \quad (A.21)$$

where $K_o = \omega_o / V_o$.

We can certainly assume $\left(\dfrac{k_z V_o D}{2 V_A} \right) \ll 1$. The integral over k_y has been done in the preceding calculation. We can apply that result to obtain

$$P_A = \frac{I_o^{\,2} V_A}{c^2} \int_0^{K_0} dk\, x \left(1 - e^{-k_z L} \right) \; \frac{\sin^2(k_z D/2)}{k_z (k_z D/2)^2} \qquad (A.22)$$

Since $K_o \ll \Omega_{ci}/V_o$, we can take $K_o D \ll 1$ so long as $D \leq 25m$. Then

$$\frac{\sin(k_z D/2)}{(k_z D/2)} \approx 1 \text{ throughout the range of integration, which gives us}$$

$$P_A = \frac{2I_o^2 V_A}{D\ C^2} \int_0^{K_0} dk_z \left(1 - e^{-k_z L}\right)\frac{\sin(k_z D/2)}{k_z^2} \qquad (A.23)$$

Again we have arrived at the very same expression as before (equation (A.11)) in the limit where $k_z D \ll 1$ except for a factor of 2. This factor could be due to a mistake we've made, but the more likely source is from equation (A.16) which we inferred from the Dobrowolny/Veltri expression (A.1).

These authors took an approach different from the one followed above. They attempted to carry through the complicated calculations using the general expression for Λ, λ_{ij}, and $\vec{e}$, only applying the Alfvén approximation at a later stage in the process.

Having written down the general formula (A.1), the authors then proceed to give results based on calculations which they characterize as "lengthy," too lengthy, evidently, to be summarized even in an appendix. Thus there is no way to follow their calculations step by step in order to judge this part of their work. They obtain (equations (13)-(15) in the original):

$$P = \frac{32 I_o^2}{\pi D^4} \sum_\sigma \int d^3k \int \frac{d\omega}{\omega} \, H\,(k,\theta,\varphi) G(k,\theta,\varphi,\omega) \delta\Big(\omega - k_x V_o\Big)$$

$$\cdot \left|\frac{\partial \Lambda}{\partial \omega}\right|^{-1} \delta\big[\omega - \omega_\sigma(k)\big] \;\; \frac{1}{k_x^2 k_y^2 k_z^2} \qquad (A.24)$$

where

$$H(k,\theta,\varphi) = \sin^2\!\Big(k_x \frac{D}{2}\Big)\sin^2\!\Big(k_y \frac{L}{2}\Big)\sin^2\!\Big(k_z \frac{D}{2}\Big) \qquad (A.25)$$

$$G(k,\theta,\varphi,\omega) = \left[\epsilon_1\epsilon_2 - n^2\Big(\epsilon_3 \cos^2\theta + \epsilon_1 \sin^2\theta\Big)\right]\cos^2\varphi +$$

$$+ \epsilon_2 \sin^2\varphi \, \frac{\big[\epsilon_3 + n^2 \sin^2\theta\big]^2}{\epsilon_1\epsilon_2 - n^2\Big(\epsilon_3 \cos^2\theta + \epsilon_1 \sin^2\theta\Big)} \qquad (A.26)$$

In formula (A.24), "the notation $\sum_\sigma$ denotes a summation over all plasma modes which are possible in the cold-plasma approximation, $\omega = \omega_\sigma(k)$ being the dispersion relation for the σ mode."

At this stage of their calculation, they insert the Alfvén wave dispersion relation into their equations.

There are two (presumably typographical) errors in the condition obtained for the angle θ that $\vec{k}$ makes with the z axis. The authors quote $\theta =$

arc $\tan\left(\dfrac{V_o}{V_A \cos \varphi}\right)$ and say that $V_A/V_o \ll 1$ implies $\theta \approx \pi/2$. In fact, $\theta =$ arc $\tan\left(\dfrac{V_A}{V_o \cos \varphi}\right)$, and the assumption (true for TSS) is $V_A/V_o \gg 1$. The expression they obtain for the Alfvén wave power is

$$P_A = \frac{32 I_o^2}{\pi D^4} \frac{V_o}{V_A} \int_o^\infty k^2\, dk \int_o^\pi \sin\theta\, d\theta \int_{-\pi/2}^{\pi/2} d\varphi \;\; \frac{1}{\omega_A(k)}$$

$$\left\{ H(k,\theta,\varphi) \cdot G(k,\theta,\varphi,\omega_A(k)) \cdot \left[\delta(\theta - \theta_1) + \delta(\theta - \theta_2)\right] \right\} \qquad (A.27)$$

The Alfvén dispersion relation is only valid for frequencies much less than the ion cyclotron frequency. Thus for the power calculation to make sense as a calculation of power into Alfvén waves, where the Alfvén dispersion relation is inserted into the integrand, the integral over ω in Equation (A.24) must be restricted to a range $|\omega| \ll \Omega_{ci}$. We note that there seems to be another typographical error in equation (A.27). Presumably a factor $\left[k_x^2 k_y^2 k_z^2 \partial \Lambda / \partial \omega \right]^{-1}$ should be included in the integrand. The more important point is that the integration over all ω has been carried out and it has not placed any limitation on the size of k_z in the integrand. If the rest of the integrand were such that only small values of k_z were important, this would not be significant; but in the orbiting wire approximation, which is later carried further to an orbiting mathematical line approximation, this cannot be valid.

At this point the authors introduce the restriction on k_x. The correctness of this step is more difficult to ascertain because of the likelihood of a typographical error in the preceding step. We did not attempt to reconstruct the calculations in full, since it would have required too many guesses about what expressions the authors were using for the dielectric tensor, etc. In any case the next step involves "very lengthy" calculations, of which no details are reported.

It is only at this stage of their calculations that Dobrowolny and Veltri begin to make approximations about the system dimensions. Their approximations are rather extreme and certainly do not correspond to a real tethered satellite system. Despite their statement near the beginning of the paper to the effect that the earlier work of Belcastro, Dobrowolny and Veltri [1982] had missed the Alfvén wings entirely because it had assumed a tether of infinite length, they proceed to make the same approximation. Not only that—they also make the extreme approximation of an orbiting wire with negligible radius. This approximation is also at odds with their previous statement that the finite size of the system was of essential importance. The point is that, by making these approximations at this later stage in the analysis, the authors have made it difficult to judge their effects. The approximations do not seem to be consistent. At one point they take $\bar{D} \equiv D\Omega_{ci}/V_o \ll 1$. Later they take $\xi_m \sim 1/\bar{D}$, which would imply $\xi_m \gg 1$, when the Alfvén condition is $\xi_m \ll 1$.

Using the $\bar{D} \ll 1$ limit (orbiting wire) they had arrived at the result ((35) in their paper)

$$P_A = \frac{I_o^2 V_o^2}{c^2 V_A} \; \bar{L} \; \xi_m \left(\frac{1}{3} \; \xi_m^2 \; + \; \frac{V_A^2}{c^2} \right) \tag{A.28}$$

They then take $\xi_m \sim \dfrac{1}{\bar{D}}$.

Now ξ_m is the maximum value of $k_z V_o / \Omega_{ci}$ allowed for the Alfvén dispersion relation to apply. It is thus necessarily much less than 1. Taking $\xi_m \sim \dfrac{1}{\bar{D}}$ violates that condition in the extreme. They then take $\xi_m \sim 1$ to obtain

$$R_A = \frac{2}{3} \left(\frac{V_A}{c^2} \right) \left(\frac{V_o}{V_A} \right)^2 \frac{L}{D} \tag{A.29}$$

as the Alfvén wave impedance.

We note that they calculated the Alfvén wave impedance at around 1Ω before this sleight of hand involving the use of $\xi_m \sim \dfrac{1}{\bar{D}}$.

Let us take their final expression (A.29) for this wave impedance and apply it to the 100 km long tethered system with a 1 mm diameter tether.

Since $L/D = 10^8$, $\frac{1}{3}\left(V_o/V_A\right)^2 \simeq 2 \times 10^{-4}$, and $\frac{2V_A}{c^2}$ corresponds to around 0.06Ω, we find $R_A \simeq 1200\Omega$!

Thus the authors seem to have made a serious mistake in obtaining their expression for the Alfvén wave impedance. Perhaps they meant to apply $\xi_m \sim 1/\overline{D}$ only to the case for which $\overline{D} \gg 1$ (though they should have said so). Then they would have obtained

$$R_A = \frac{2}{3} \frac{V_A}{c^2} \left(\frac{V_o^2}{V_A}\right)^2 \frac{L}{\Omega_{ci}^2 D^3} \qquad (A.30)$$

(assuming $\frac{1}{\overline{D}^2} \gg \frac{V_A^2}{c^2}$).

But this expression is unlike any previous results and differs from that of Drell, et al. by a factor $\frac{1}{3}\left(\frac{V_o^2}{V_A\Omega_{ci}D}\right)^2$.

Dobrowolny and Iess have not really argued that the quadratic dependence obtained by them is the correct one, only that a dependence on the velocity that clearly vanishes as the velocity goes to zero is necessary. There is no disagreement on this point. The time variation in the problem is strictly due to the relative motion between the satellite system and the magneto-plasma, so there would be no waves excited by a motionless tethered satellite, should such a system

be possible. As we shall demonstrate, the SAO calculation also gives a null result when the velocity is zero. It is also plausible that the Alfvén wave impedance should not otherwise depend on the velocity, so that the "physical" argument for the Dobrowolny/Veltri result turns out to be weak.

We have now arrived at the SAO expression three different ways, but let us examine the two parts of the criticism of the SAO results made by Dobrowolny and his colleagues. First, let us consider their assertion that the SAO results cannot be correct because they do not go to zero with the system's velocity. This assertion is demonstrably false. Consider our expression for the Fourier transform of E_y (equation (18) in our JGR paper). It contains the factors $\omega\delta(\omega - k_x v_x)$. This is to be integrated over ω. Now the fundamental, defining property of the Dirac delta function is

$$\int f(\omega)\delta(\omega - \omega_o)\,d\omega = f(\omega_o)$$

Thus when we take the inverse Fourier transform to obtain E_y, which contains a linear factor of ω, we obtain zero if the satellite velocity is zero. All subsequent calculations thus assume that the satellite velocity is not zero, for indeed there are no waves generated in the zero velocity case. Thus for Dobrowolny and his colleagues to take us to task for failing to have an explicit dependence on the satellite velocity in all our subsequent results, which are various limiting cases (all

of which assume a non-zero satellite velocity), is unfair.

Iess has maintained that, if one first does the inverse Fourier integration and <u>then</u> takes the limit as v_z goes to zero, the SAO expression for the wave impedance does not go to zero. It is easy to demonstrate that one cannot expect always to get the same result by inverting the order of integration and limit taking. Consider

$$f(\omega, x) = \frac{\omega \; \delta(\omega - \omega_o)}{x^2 + \omega_o{}^2}$$

and take the integral over all ω and x.

$$\int f(\omega, x) \, dx \, d\omega = \int \frac{\omega_o}{x^2 + \omega_o{}^2} \, dx = \pi,$$

which is independent of ω_o. But it has already been assumed that ω_o is not zero, so that taking the limit as ω_o goes to zero after the integration is nonsensical. In physical calculations we must always be guided by the physics in deciding "mathematical" questions; as, for example, causality is frequently invoked to determine contour integration paths. Let us apply physical reasoning to the case at hand. What is the source of the ω factor in our integrand? It corresponds to a time derivative. What is the source of the $\delta(\omega - k_z v_z)$ factor? It comes from the <u>physical</u> condition that the only time variation in the problem is due to the

motion of the system with respect to the plasma. Thus taking v_z to be zero before integration is the choice that makes physical as well as mathematical sense.

Finally, we note again that Dobrowolny and Veltri concentrate on explaining their differences with the results of Drell et al. presumably because both analyses found a similar dependence on the tethered systems' dimensions.

They do not discuss why the Drell formula's linear variation with the tether length and inverse variation with the system's dimension along the direction of motion should apply to the case they had considered at all, since Rasmussen et al. [1985] had already pointed out that the Drell results did not apply to a tethered system. In fact, Chu and Gross in 1966 ascertained that the Drell results were not applicable to any system having a vertical dimension that was not much smaller than its dimension along the direction of motion, i.e. just the opposite situation from what applies in the case of a tethered satellite.

REFERENCES for Appendix

Chu, C.K., and R.A. Gross, Alfvén waves and induction drag on long cylindrical satellites, *AIAA* Journal 4, 2209, 1966.

Gradshteyn, I.S., and I.M. Ryzhik, *Table of Integrals, Series, and Products*, Academic Press, New York, 1980.

Melrose, D.B., *Plasma Astrophysics*, Vol. 1, Gordon and Breach Science Publishers, New York, 1980.